Local contributions to infiltration excess runoff for a conceptual catchment scale model

Stefano Orlandini and Marco Mancini

Dipartimento di Ingegneria Idraulica, Ambientale e del Rilevamento, Politecnico di Milano, Milan, Italy

Claudio Paniconi

Centro di Ricerca, Sviluppo e Studi Superiori in Sardegna, Cagliari, Italy

Renzo Rosso

Dipartimento di Ingegneria Idraulica, Ambientale e del Rilevamento, Politecnico di Milano, Milan, Italy

Abstract. The response of a conceptual soil water balance model to storm events is compared to a detailed finite element solution of the one-dimensional Richards equation in order to test the capabilities of the former in calculating the local contributions to infiltration excess runoff in a distributed catchment scale model. Local infiltration excess runoff is computed from ground level precipitation using the time compression approximation and a Philip infiltration capacity curve with Brooks-Corey constitutive equations. The validity of applying the conceptual model for local runoff and soil water balance calculations is investigated by performing numerical experiments over a range of soil types, control volume depths, and initial soil moisture conditions. We find that a good agreement between the conceptual and detailed models is obtained when the gravitational infiltration rate in Philip's formula is set to the saturated hydraulic conductivity, and when percolation from the control volume is updated as a function of the soil moisture content in a stepwise fashion. The comparison between these two models suggests that the simpler (and much less computer-intensive) conceptual water balance technique could be incorporated into distributed models for large scale complex terrains as an efficient means of retaining consideration of spatial variability effects in catchment scale hydrologic simulations. This is illustrated in an application to the Rio Missiaga catchment in the eastern Italian Alps, where the local contributions to surface and subsurface runoff are routed onto a digital elevation model–based conceptual transport network via a simple numerical scheme based on the Muskingum-Cunge method.

1. Introduction

Scientists and engineers who must make decisions based on hydrologic information have made remarkable progress in their efforts to develop and use models that enable them to predict streamflow rates in response to storm events. Although it was once sufficient to model catchment outflow, it is now often necessary to estimate distributed surface and subsurface flow characteristics as driving mechanisms for erosion, sedimentation, chemical and nutrient transport, and other spatially distributed effects [*Abbott et al.*, 1986]. The integration or linkage of a distributed hydrologic model with the spatial data-handling capabilities of digital elevation models (DEMs) and digital terrain models (DTMs) offers advantages associated with utilizing the full information content of spatially distributed data to analyze hydrologic processes.

Richards' equation–based numerical models have been used in the past to simulate hillslope and catchment scale hydrologic processes [*Freeze*, 1971; *Smith and Hebbert*, 1983; *Binley et al.*, 1989; *Paniconi and Wood*, 1993]. For large scale catchment simulations the computational resources needed to run de-tailed models may be excessive, creating a need for simpler conceptual techniques which embody the essential concepts of component subprocesses while also allowing space-time variability to be considered. Detailed physically based models have proven useful in evaluating the underlying assumptions in conceptual models. Examples of such studies can be found in work by *Gan and Burges* [1990] (rainfall-runoff models on small hypothetical catchments), *Sloan and Moore* [1984] (one- and two-dimensional subsurface storm flow models), *Ibrahim and Brutsaert* [1968] and *Reeves and Miller* [1975] (one-dimensional infiltration models to test the time compression approximation), and *Troch et al.* [1993] (water table dynamics, soil moisture profiles, and subsurface flow contributions to stream discharge in a conceptual water balance model).

Protopapas and Bras [1991] examined the feasibility of using a simplified representation of a heterogeneous soil medium in infiltration models. Within the limits of the assumptions used in their study they found that for uniform application of water at the surface, the heterogeneous medium can be represented by a set of noninteracting soil columns. *Salvucci and Entekhabi* [1994a, b] investigated the validity of representing the soil moisture profile with two layers of different depths. Under deep water table conditions the soil profile is shown to be very sensitive to climatically forced moisture changes for the upper 10 cm, whereas the lower "transmission" zone is much less

responsive. For shallow water table conditions the soil profile can no longer be conceptually divided into a highly unsteady zone and a quasi-steady zone. Scaling such results from a one-dimensional analysis to larger areas where spatial inhomogeneity and lateral hydrologic processes can be important is a nontrivial task [*Milly and Eagleson*, 1987; *Entekhabi and Eagleson*, 1989; *Famiglietti and Wood*, 1994].

In this paper we develop a simple and computationally inexpensive conceptual model that incorporates atmospheric storm and interstorm forcing, vegetation, and soil moisture and hydraulic properties to estimate the local contributions to infiltration excess runoff at the DEM elemental cell scale. In particular, we focus on the water balance of the upper soil layer during storm events. This layer plays a critical role in rainfall-runoff modeling, and adequately simulating its dynamics in detailed numerical models can incur great computational expenses, owing to rapid response in this zone to atmospheric forcing, which constrains such models to small grid and time step sizes. This motivates a need for simplifying the description of the land surface moisture dynamics through the introduction of conceptual models.

The soil response of the conceptual model developed in this study is evaluated against a detailed numerical model in order to investigate the possible use of the simpler technique in distributed models for large scale complex terrains as an efficient means of retaining consideration of land surface spatial variability effects in catchment scale hydrologic simulations. One of the long term objectives is to couple the conceptual one-dimensional representation of the upper soil zone to a more detailed three-dimensional model for the lower soil zones, where lateral hydrologic processes can be important and where numerical constraints are less stringent. A different strategy for coupling unsaturated and saturated flows has been considered by *Salvucci and Entekhabi* [1995] in the development of a statistical-dynamical methodology for hydrologic simulation at the climatic timescale.

The catchment scale water balance model is designed to capture the broad features of hydrologic response for steeply sloping terrains and heavy storm events. These climatic and topographic conditions are representative of many catchments in the northern and central mountainous regions of Italy. In these regions infiltration excess is the dominant surface runoff production mechanism for lowland areas, where fine-grained sedimentation results in relatively low surface hydraulic conductivities, although strong subsurface kinematic storm flow response from the coarse-grained upland areas can also occur during extreme storm events. The use of the model is illustrated in an application to the 4.35-km^2 Rio Missiaga experimental catchment, where we compare simulated and observed outlet discharge measurements. In this application the model is coupled to a simple integration scheme based on the Muskingum-Cunge method. Topographic control on downslope water movement is treated by processing each of the DEM cells, from upland areas to the basin outlet, through a conceptual transport network extracted from DEM data.

2. Local Scale Runoff at Two Levels of Conceptualization

The classical Richards equation describing fluid motion in the unsaturated zone may be written in several forms, with either soil matrix potential ψ or moisture content θ as dependent variable. The constitutive relationship between ψ and θ

allows for conversion of one form of the equation to another. The one-dimensional Richards equation with pressure head as the dependent variable can be written as

$$\sigma(\psi) \frac{\partial \psi}{\partial t} = \frac{\partial}{\partial z} \left[K_s K_r(\psi) \frac{\partial(\psi + z)}{\partial z} \right], \qquad (1)$$

where $\sigma(\psi) = d\theta/d\psi$ is the specific moisture capacity, t is time, z is the vertical coordinate (positive upward), and the hydraulic conductivity is expressed as a product of the conductivity at saturation, K_s, and the relative conductivity, $K_r(\psi)$. The Brooks-Corey characteristic equations [*Brooks and Corey*, 1966] can be used to describe the nonlinear dependencies of θ, K_r, and σ on ψ:

$$\theta(\psi) = \theta_r + (\theta_s - \theta_r)\left(\frac{\psi_s}{\psi}\right)^\eta \qquad \text{if } \psi \le \psi_s$$
$$\theta(\psi) = \theta_s \qquad \text{if } \psi > \psi_s, \qquad (2)$$

$$K_r(\psi) = \left(\frac{\psi_s}{\psi}\right)^{2+3\eta} \qquad \text{if } \psi \le \psi_s$$
$$K_r(\psi) = 1 \qquad \text{if } \psi > \psi_s, \qquad (3)$$

$$\sigma(\psi) = \frac{\eta(\theta_s - \theta_r)}{|\psi_s|}\left(\frac{\psi_s}{\psi}\right)^{\eta+1} \qquad \text{if } \psi \le \psi_s$$
$$\sigma(\psi) = 0 \qquad \text{if } \psi > \psi_s, \qquad (4)$$

where θ_r is the residual moisture content, θ_s is the saturated moisture content, ψ_s is the saturated soil matrix potential, and η can be interpreted as a pore size distribution index. Hysteresis effects on moisture redistribution in the soil profile are not taken into account.

Two local physically based infiltration excess models are considered in this study, both of which can be classed as deterministic conceptual type models [*Clarke*, 1973]: a time compression approximation–based (TCA) water balance model of the upper unsaturated soil layer (the "conceptual TCA" model) and a detailed Richards' equation based one-dimensional finite element model (the "detailed numerical" model).

2.1. Conceptual TCA Model

The conceptual model considered in this study to calculate the local infiltration excess runoff is part of a model structure that is designed to provide an integrated representation of the soil-vegetation-atmosphere continuum at the topographic scale represented by digital elevation data and terrain attributes [*Orlandini*, 1995]. The local water balance is performed by calculating the vertical water fluxes between soil, vegetation, and atmosphere during storm-interstorm sequences so that the vegetation canopy and soil moisture status can be updated in a stepwise fashion (Figure 1). In this paper we focus on the nonlinear response of the upper soil layer to storm events. The water balance of the upper unsaturated soil layer during storm periods is expressed by the continuity equation

$$Z_{\text{up}} \frac{d\theta_{\text{up}}}{dt} = f_i - g, \qquad (5)$$

where Z_{up} is the control volume depth, θ_{up} is the average volumetric water content of the soil control volume, f_i is the actual infiltration rate, and g is the percolation rate to the
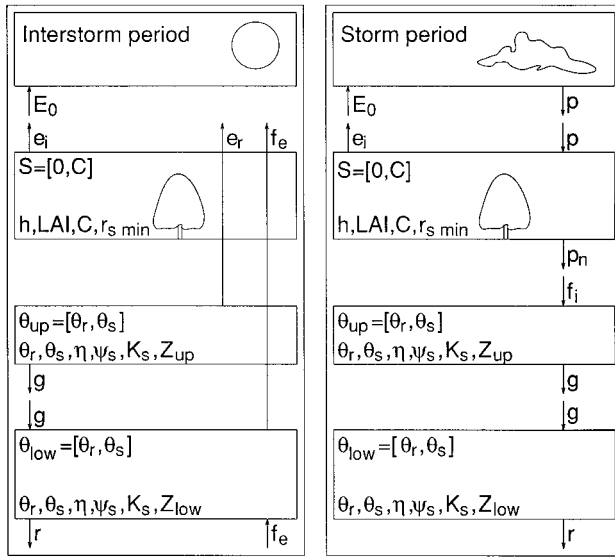
Figure 1. Conceptualization of the soil-vegetation-atmosphere continuum. S, canopy storage; C, canopy storage capacity; h, canopy height; $r_{s\ min}$, minimum crop resistance to water vapour transfer; LAI, leaf area index; θ_{up} and θ_{low}, average volumetric water contents of the upper and lower soil layers; θ_r and θ_s, residual and saturated volumetric soil water contents; η, pore size distribution index; ψ_s, saturated soil matrix potential; K_s, saturated hydraulic conductivity; Z_{up} and Z_{low}, upper and lower soil layer depths; E_0, potential evaporation; e_r, evaporation from the root zone; p, precipitation; p_n, ground level precipitation; e_i, evaporation from the wetted canopy; f_i and f_e, infiltration and exfiltration; g, percolation to the transmission zone; and r, local contribution to subsurface flow.

lower soil layers. Soil hydraulic properties and moisture status are incorporated into the model via the Philip infiltration capacity equation and the Brooks-Corey relationship [*Philip*, 1960; *Eagleson*, 1978]. The infiltration capacity is expressed as

$$f_{i*}(t) = \frac{1}{2} S_i t^{-1/2} + A_i, \tag{6}$$

where the parameters S_i and A_i are known as the sorptivity and gravitational infiltration rate, respectively. Following the derivation described by *Eagleson* [1978], the expression for S_i is

$$S_i = 2(\Theta_0 - \Theta_i) \left[\frac{5\theta_s |\psi_s| K_s \phi_i(\delta, \Theta_i)}{3\eta\pi} \right]^{1/2}, \tag{7}$$

where $\Theta = (\theta - \theta_r)/(\theta_s - \theta_r)$ is the reduced soil water content, Θ_i and Θ_0 are the initial and land surface saturation values, $\delta = (1 + 2\eta)/\eta$, and $\phi_i(\delta, \Theta_i)$ is a dimensionless parameter defined as

$$\phi_i(\delta, \Theta_i) = (\Theta_0 - \Theta_i)^{-5/3} \int_{\Theta_i}^{\Theta_0} \Theta^\delta (\Theta - \Theta_i)^{2/3} d\Theta. \tag{8}$$

The initial condition of soil saturation Θ_i in (7) is expressed as

$$\Theta_i = \frac{Z_{up}}{Z_{up} + Z_{low}} \Theta_{up\ i} + \frac{Z_{low}}{Z_{up} + Z_{low}} \Theta_{low\ i}, \tag{9}$$

where Z_{up}, Z_{low}, $\Theta_{up\ i}$, and $\Theta_{low\ i}$ are the control volume depths and the initial saturation values for the upper and lower

layers. The land surface boundary condition during storm events is assumed to be $\Theta_0 = 1$.

We found that the best agreement between conceptual TCA and detailed numerical models is obtained when the gravitational infiltration rate in equation (6) is set to K_s, the saturated hydraulic conductivity, that is, when

$$A_i = K_s. \tag{10}$$

The percolation rate g to the lower soil layer is expressed by extrapolating the Brooks-Corey constitutive equations (2) and (3) from the point to the finite control volume scale, via the storage-outflow relationship

$$g = \max(f_i, K_s) \Theta^{(2+3\eta)/\eta}, \tag{11}$$

so that the nonlinear control volume behavior is expressed as a function of the hydraulic soil properties. The factor $\max(f_i, K_s)$ is introduced to account for soil percolation when the actual infiltration rate is less than the saturated soil conductivity. It is one of the principal aims of this paper to verify the ability of (11) to calculate the upper soil control volume outflow and thus the water balance of this zone.

Equation (5) is solved numerically during the storm event by applying two levels of discretization (Figure 2). At the first level the storm simulation period $[0, T]$ is divided into M intervals $[(m - 1)\Delta T, m\Delta T](m = 1, \cdots, M)$, and at the mth time interval the average value of the atmospheric input variables are considered. At the second level of discretization the generic time interval $[(m - 1)\Delta T, m\Delta T]$ is divided into K subintervals $[(k - 1)\Delta t, k\Delta t](k = 1, \cdots, K)$, where $\Delta t = \Delta T/K$, so that (5) can be solved numerically from the initial condition $\theta_{up}^{m,0} = \theta_{up}^{m-1}$ by applying a simple explicit forward Euler scheme
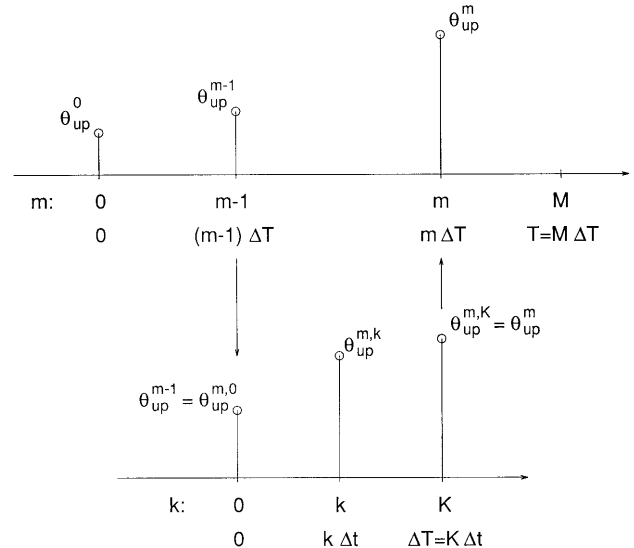
Figure 2. Discretization of the simulation time domain. With reference to the upper layer soil moisture content θ_{up}, shown is how the simulation period $[0, T]$ is divided into M intervals ΔT to perform the time compression approximation (TCA) between atmospheric forcing and soil characteristics, and how each interval ΔT is further subdivided into K subintervals Δt to resolve the nonlinear water balance equation. From a computational point of view the program can store moisture status at each time step m ($m = 0, \cdots, M$) and average fluxes over each time interval $[(m - 1)\Delta T, m\Delta T]$.

$$\theta_{\mathrm{up}}^{m,k} = \theta_{\mathrm{up}}^{m,k-1} + \frac{1}{Z_{\mathrm{up}}} (f_i^{m,k-1} - g^{m,k-1})\Delta t, \qquad (12)$$

where the average value of the actual control volume infiltration rate $f_i^{m,k-1}$ can be calculated via a TCA that considers the interaction between ground level input p_n and the infiltration capacity f_{i*}, so that

$$f_i^{m,k-1} = \min{(p_n^{m,k-1}, f_{i*}^{m,k-1})}, \qquad (13)$$

where $f_{i*}^{m,k-1}$ has been expressed as a function of the cumulative infiltration depth $F_i(t) = \int_0^t f_i(\tau)\, d\tau$ according to *Milly* [1986]:

$$f_{i*} = \frac{S_i^2}{2F_i}, \quad A_i = 0 \qquad (14)$$

$$f_{i*} = A_i \left\{ 1 + \left[-1 + \left(1 + \frac{4A_i F_i}{S_i^2} \right)^{1/2} \right]^{-1} \right\}, \quad A_i > 0. \qquad (15)$$

The value $g^{m,k-1}$ in (12) is estimated via (11) as a function of the moisture content $\theta_{\mathrm{up}}^{m,k-1}$. For the mth time interval the soil moisture content $\theta_{\mathrm{up}}^{m,K} = \theta_{\mathrm{up}}^m$ is derived by solving (12) from the initial condition $\theta_{\mathrm{up}}^{m,0} = \theta_{\mathrm{up}}^{m-1}$. The mean values of the inflow f_i and outflow g are taken to be

$$f_i^m = \frac{1}{\Delta T} \sum_{k=1}^{K} \frac{1}{2} (f_i^{m,k-1} + f_i^{m,k})\Delta t, \qquad (16)$$

$$g^m = \frac{1}{\Delta T} \sum_{k=1}^{K} \frac{1}{2} (g^{m,k-1} + g^{m,k})\Delta t. \qquad (17)$$

Water balances similar to those expressed by (5) can be solved for each control volume represented in Figure 1, during storm-interstorm sequences, to yield moisture status and response fluxes [*Orlandini*, 1995].

As reported by *Salvucci and Entekhabi* [1994a], the estimation of the sorptivity S_i given by (7) applies only for soil saturation Θ less than 1 and soil matrix potential ψ less than the saturated value, ψ_s. During storm events a tension-saturated zone, where $\psi_s \leq \psi \leq 0$, will generally develop prior to ponding and thus must be modeled in the derivation of infiltration capacity. *Philip* [1958] noted that the effect of the tension-saturated zone is equivalent to that of ponded water of depth $|\psi_s|$ at the soil surface, and he showed that its effect on infiltration capacity could be accounted for by modifying the sorptivity S_i, as

$$S_{i,\mathrm{mod}} = [S_i^2 + 2\theta_s K_s |\psi_s|(1 - \Theta_i)]^{1/2}. \qquad (18)$$

If we omit this correction when the soil is initially unsaturated, the capillary term $1/2 S_i t^{-1/2}$ in (6) is underestimated. This effect is dampened as the soil tends to saturation. On the other hand, for unsaturated soils the gravitational term A_i in (6), when set to K_s as per (10), is overestimated with respect to the unsaturated hydraulic conductivity $K(\Theta) = K_s \Theta^{(2+3\eta)/\eta}$, and this overestimation is reduced as the soil tends to saturation. Therefore the underestimation of S_i in (7) and the overestimation of A_i in (10) tend to compensate each other, yielding a solution that is asymptotically correct as the soil tends to saturation and that provides a good estimate of the capillary effect at the beginning of the infiltration process for any initial condition of soil saturation, Θ_i. This treatment is also consistent

with the TCA procedure represented by (13)–(15), which requires that both S_i and A_i be constant in time.

We make some remarks here on the physical reasoning underlying (11). The description of the drainage process from a control volume formulation is not a trivial task since this formulation implies that we lose information on the soil moisture profile and therefore on the soil matrix potential gradient that contributes to the Darcian flux at the control volume base

$$g_D = -K(\psi) \frac{\partial}{\partial z} (z + \psi). \qquad (19)$$

Previous conceptual hydrologic models [e.g., *Famiglietti and Wood*, 1994] have used $g = K_s \Theta_{\mathrm{up}}^{(2+3\eta)/\eta}$ to estimate the drainage, neglecting $\partial \psi/\partial z$ at the base boundary of the soil control volume. This leads to overestimation of the drainage flux during interstorm periods (when $f_i = 0$) and underestimation during storm events. During storm events, information on capillary effects is included in the term f_i, and we make use of this information to estimate the drainage flux g, introducing the factor $\max(f_i, K_s)$ in (11). The control volume water balance described by (11)–(13) is "computationally stable" in the sense that errors in the control volume moisture content due to incorrect estimates of g for a time interval Δt produce in subsequent intervals errors in the drainage estimate that tend to correct the water balance. The role of the forcing factor f_i in this feedback is crucial. As far as we know, the problem of control volume drainage prediction during interstorm periods is still not completely resolved.
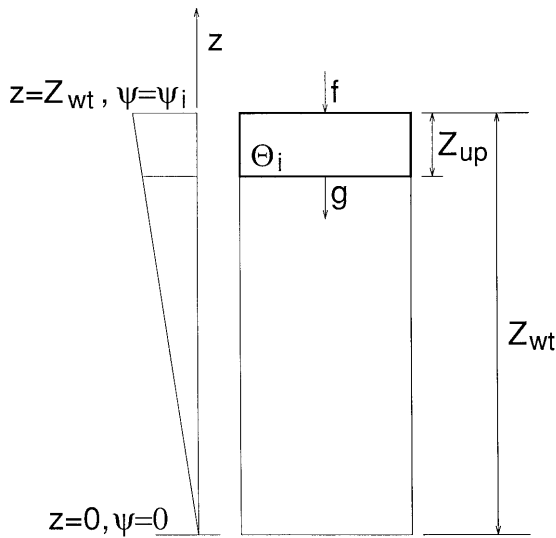
2.2. Detailed Numerical Model

The numerical model described by *Paniconi et al.* [1991] is used to calculate a reference water balance for the upper soil layer. A finite element Galerkin discretization in space and a finite difference discretization of the time derivative term is used to solve (1). The resulting system of nonlinear equations is linearized using either Picard or Newton iteration, and a "back-stepping" procedure is applied to resize the time interval when convergence is not reached in an assigned number of iterations. The model incorporates the Brooks-Corey constitutive equations (2)–(4) and numerically solves the one-dimensional Richards equation over a specified time period for a given set of boundary and initial conditions.

The potential inflows to the model consist of precipitation and evaporation flux inputs at the top of the soil column. The actual (simulated) inflows are determined according to the type of boundary condition imposed, and during simulation the model automatically adjusts this boundary condition according to changes in pressure head and flux values at the surface. When the potential flux is positive, the difference between potential and actual soil inflow is the surface runoff. Surface runoff is produced when the infiltration capacity of the soil falls below the rainfall rate (infiltration excess mechanism) or when the soil column becomes completely saturated (saturation excess mechanism). The boundary condition at the surface when runoff occurs switches from a Neumann type (atmosphere-controlled inflow) to a Dirichlet type (soil-controlled inflow).

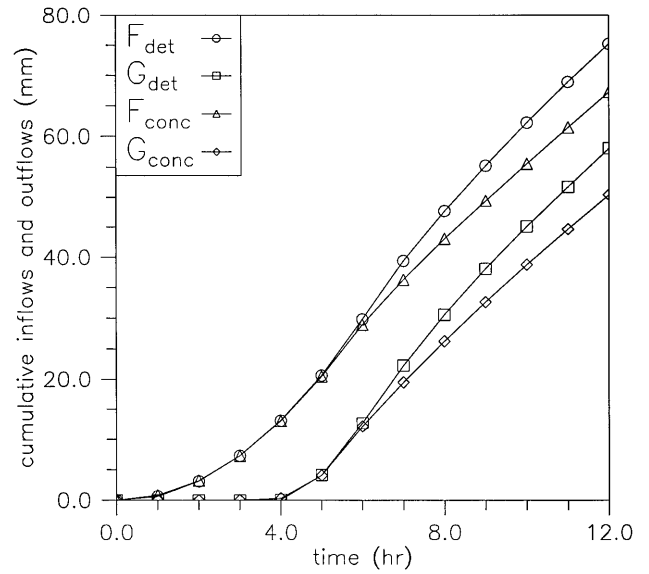## 3. Comparison Between Conceptual and Detailed Water Balance Models

To compare the capabilities of the conceptual TCA and detailed numerical models to calculate local contributions to

Figure 3. Sketch of the soil control volume at the beginning of the simulation for comparing the detailed and conceptual models. The conceptual TCA water balance is referred to the upper soil layer of depth Z_{up}, and the numerical model computations are performed over the entire soil column of depth Z_{wt}, in order to make the influence of the base boundary condition negligible on that model's calculated outflow flux g.

Figure 4. Comparison between detailed and conceptual water balance models. The simulated control volume cumulative inflows F and outflows G are plotted for the base case parameter set of Table 1, except with $Z_{up} = 0.10$ m.

infiltration excess runoff, water balance simulations are performed for the upper unsaturated soil layer. The soil control volume has depth Z_{up} and is represented in Figure 3. The uniformly wetted initial soil profile, $\Theta = \Theta_i$, assumed for the conceptual model is approximated for the detailed model by a linear soil matrix potential distribution, from $\psi = 0$ at the water table ($z = 0$) to $\psi = \psi_i$, where $\psi_i = \psi(\Theta_i)$, at the land surface ($z = Z_{wt}$). This approximation is reasonable when the control volume depth Z_{up} is much smaller than the soil column depth Z_{wt}. The validity of this approximation for larger control volume depths and the effects of various initial distributions, including uniform and hydrostatic conditions, will be investigated in future work. In addition to the control volume inflow f, the outflow flux g is also compared between the two models, in order to evaluate the conceptual model's ability to simulate the percolation to the lower soil layers and, from (5), the updating of the land surface soil water status.

As described in section 2, both the conceptual TCA and detailed numerical models are based on the same set of soil hydraulic properties: K_s and the parameters θ_r, θ_s, η, and ψ_s of the Brooks-Corey constitutive equations (2)–(4). In addition to these soil parameters, initial and land surface boundary conditions of soil saturation, Θ_i and Θ_0, also affect the soil water balance calculations. In this study we examine the sensitivities of the conceptual model response to scale representation, soil type, and initial moisture status, selecting Z_{up}, K_s, and Θ_i as representative parameters. On the basis of past studies with detailed models, it is known that K_s and Θ_i are critical parameters in infiltration and runoff simulations [*Paniconi and Wood*, 1993; *Troch et al.*, 1993]. In addition to these two parameters, the influence of Z_{up} is important as it underlies the idea of separating the soil profile into upper and lower components, eventually coupling the conceptual model's treatment of the upper zone to a more detailed modeling of the lower zone. Finally, important assumptions about Z_{up} and Θ_i

are made in deriving the Philip equations which form the basis of the conceptual TCA model.

The quantitative comparison between conceptual and detailed models is performed by considering a synthetic hyetograph as the input forcing term p_n and calculating the relative error on the cumulative inflow and outflow fluxes at the end of the simulation period T,

$$\varepsilon F = \frac{F_{det} - F_{conc}}{F_{det}}, \tag{20}$$

$$\varepsilon G = \frac{G_{det} - G_{conc}}{G_{det}}, \tag{21}$$

where $F = \int_0^T f\, dt$, $G = \int_0^T g\, dt$, and the subscripts "det" and "conc" denote the detailed and conceptual model results, respectively (Figure 4), over a range of soil control volume depths, Z_{up}, soil saturated hydraulic conductivities, K_s, and reduced soil moisture content initial conditions, Θ_i. The base case parameter set for the runs is given in Table 1. In Figures 5, 6, and 7 the parameters Z_{up}, K_s, and Θ_i, respectively, are varied, keeping all other parameters fixed.

The forcing hyetograph represents a ground level precipitation rate which is constant over each time interval $\Delta T = 1$ hour. The storm intensity p_n ranges from 0 to 20 mm hr^{-1} over
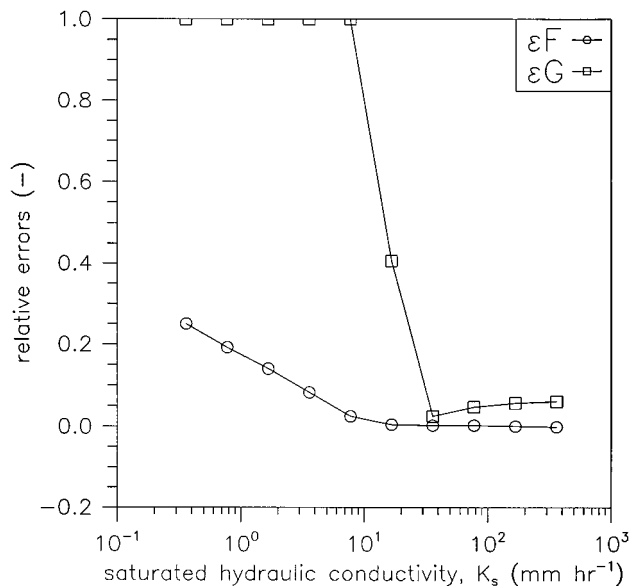
Table 1. Base Case Parameter Set for Comparing the Conceptual and Detailed Model Responses

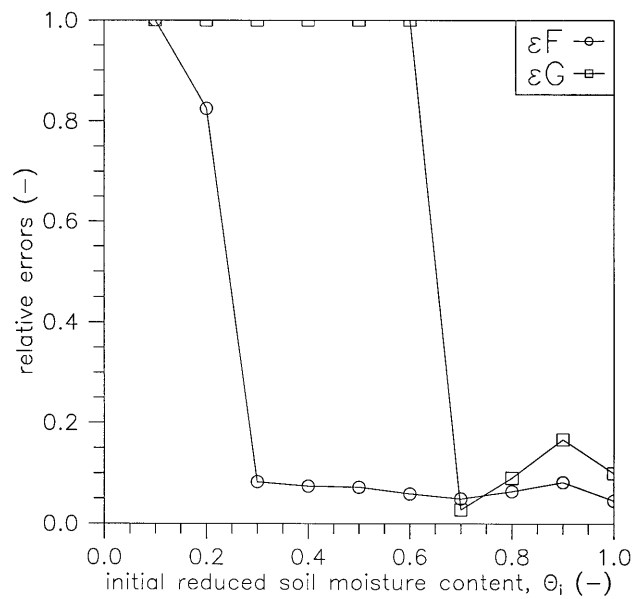| Parameter	Value
Θ_i	0.30
θ_r	0.10
θ_s	0.50
η	0.30
ψ_s, m	0.15
K_s, mm hr^{-1}	3.60
Z_{up}, m	0.40
Z_{wt}, m	4.00
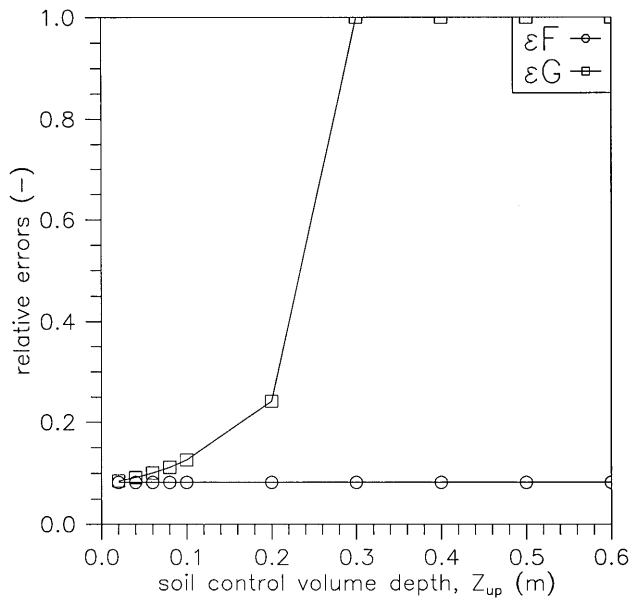
Figure 5. Comparison between detailed and conceptual water balance models. The relative errors in the cumulative inflow, εF, and outflow, εG, are plotted for a range of soil control volume depths Z_{up}.

Figure 7. Comparison between detailed and conceptual water balance models. The relative errors in the cumulative inflow, εF, and outflow, εG, are plotted for a range of initial soil moisture normalized conditions Θ_i.

the 12-hour simulation period T, and the cumulative rainfall over the simulation period is $P = 240$ mm. For some of the parameter combinations used in the results shown in Figures 5–7, the detailed numerical model neither converged (e.g., for very small values of initial soil moisture content) nor produced outflow G over the simulation period T (e.g., for large control volume depths, low conductivity, or very dry initial profile). At these points we consider the relative errors εF or εG to be maximal in some sense, and they are assigned a value of 1.0 in the plots of Figures 5–7.


Figure 6. Comparison between detailed and conceptual water balance models. The relative errors in the cumulative inflow, εF, and outflow, εG, are plotted for a range of soil saturated hydraulic conductivities K_s.

The relative errors with respect to soil control volume depth are shown in Figure 5. The cumulative inflow is not sensitive to Z_{up}. On the other hand, the cumulative outflow is highly sensitive to Z_{up}, with smaller differences between the two models observed for smaller Z_{up}. Large differences between the conceptual and detailed model outflow fluxes are seen for $Z_{\text{up}} > 0.10$ m, and this indicates that the assumption of uniform initial soil profile used in the conceptual model becomes less valid as the depth of this upper soil layer is made too large, in relation to the depth of the entire unsaturated soil column (see Figure 1). A similar interpretation can be given to the results shown in Figure 6, where we see that the largest errors, in both inflow and outflow fluxes this time, occur at low saturated conductivity. When K_s is low the effect of the $K_r(\psi)\partial(\psi + z)/\partial z$ term in (1) is enhanced, producing different results for the different initial $\psi(\Theta_i)$ profiles used in the conceptual and detailed models. On the other hand, we note that in Figures 5 and 6 the initial saturation value for the profile is $\Theta_i = 0.30$ (Table 1), which represents a fairly dry initial soil profile. In Figure 7 we observe that for wetter initial soil profiles the agreement between the two models improves, even though the combination of Z_{up} (0.40 m) and K_s (3.60 mm hr^{-1}) used in Figure 7 yielded disagreements in Figures 5 and 6. We conclude that for initial profiles which are not too dry the agreement between the conceptual and detailed models is satisfactory. Note that these are also conditions under which the local contributions to subsurface storm flow from the transmission zone are important. Under dry initial conditions, good agreement between the models is obtained when the upper soil layer is shallow or permeable. We stress that the conditions under which the conceptual and detailed models are similar are not limited to small control volume with high saturated hydraulic conductivity and wet initial soil profiles. Figures 5, 6, and 7 show the variability of the test results when one parameter is varied while the others are kept fixed. Since the base case parameter set of Table 1 was chosen with reference to severe conditions
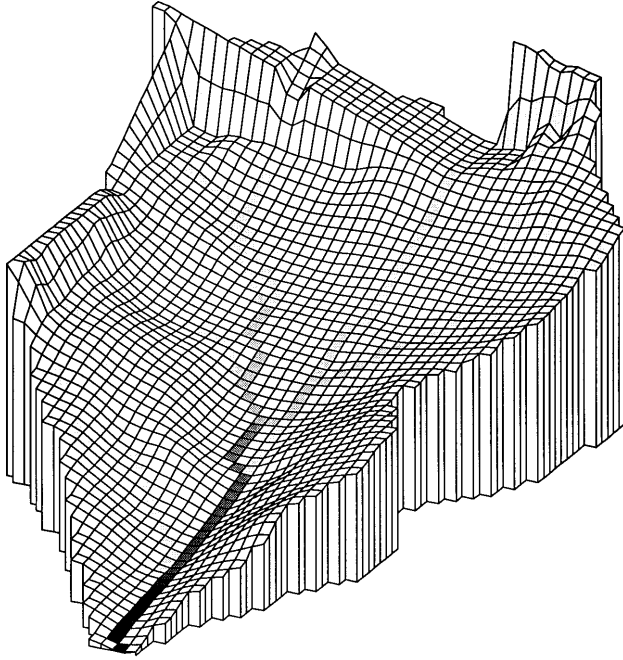
Figure 8. The 50 m × 50 m resolution digital elevation model (DEM) of the Rio Missiaga experimental catchment showing the network ordering system, with the darker shades representing higher cell-channel orders.

of simulation ($Z_{up} \gg 0.10$ m, $K_s \ll 36$ mm hr^{-1}, and $\Theta_i \ll 0.70$), these figures show that the soil dynamics are reasonably well reproduced under quite lax conditions on two of the three parameters, while the third parameter may be more restricted (e.g., $Z_{up} \leq 0.10$ m with $K_s = 3.60$ mm hr^{-1} and $\Theta_i = 0.30$).

The simulation results suggest that relation (11) can be generally applied to perform the water balance of a two-layer unsaturated soil profile during storm periods by using a thin control volume layer to simulate the highly dynamical water flux partitioning at the land surface, and a thicker layer to simulate the quasi-steady dynamics of the lower transmission zone. The model comparisons carried out in this study break down, especially for drainage estimates, when we consider the combination of soil control volumes deeper than 0.10 m, low conductivities ($K_s \leq 3.60$ mm hr^{-1}), and dry conditions ($\Theta_i \leq 0.30$). These are circumstances in which the transmission role of the control volume is not important.

4. Runoff Routing

The infiltration excess runoff produced by the conceptual TCA model is routed onto a distributed transport network, whose local channel geometry depends on the DEM cell locations. Following *Band* [1986], each of the grid cells of the basin are characterized by a maximum-slope pointer, and the network links are organized into a stream-ordering system extracted from the DEM data (Figure 8). According to the *Leopold and Maddock* [1953] self-similarity downstream relationships, the rectangularly shaped elemental channels of the network are assumed to have a width that depends on the upstream drainage area [*Orlandini and Rosso*, 1996].

The effects of topography on surface and subsurface runoff routing are incorporated through the DEM data. A given grid cell will receive water from its upslope neighbors and discharge

to its downslope neighbor according to the network ordering system described above. Inflow hydrographs and local contributions are routed onto each individual grid cell channel via the Muskingum-Cunge scheme [*Cunge*, 1969]

$$Q_{i+1}^{j+1} = C_1 Q_i^{j+1} + C_2 Q_i^j + C_3 Q_{i+1}^j + C_4 q_{Li+1}^{j+1}, \qquad (22)$$

where Q_{i+1}^{j+1} is the discharge at network link point $(i+1)\Delta s$ and time $(j+1)\Delta t$; q_{Li+1}^{j+1} is the lateral inflow due to the local contribution to infiltration excess runoff at the $(i+1)$th space interval and $(j+1)$th time interval; and the coefficients C_1, C_2, C_3, and C_4 are functions of the wave celerity c_k, the space-time interval sizes, and the weighting factor X used in the Muskingum-Cunge method for discretizing the kinematic flow equation

$$\frac{\partial Q}{\partial t} + c_k \frac{\partial Q}{\partial s} = c_k q_L. \qquad (23)$$

By assuming that the numerical diffusion in the Muskingum-Cunge method is equal to the hydraulic diffusion D_h in the diffusion-convection flow equation

$$\frac{\partial Q}{\partial t} + c_k \frac{\partial Q}{\partial s} = D_h \frac{\partial^2 Q}{\partial s^2} + c_k q_L, \qquad (24)$$

X can be expressed as a function of flow width B, channel bed slope S_o, and the three-point average discharge $\bar{Q} = (Q_i^j + Q_{i+1}^j + Q_i^{j+1})/3$ [*Ponce and Yevjevich*, 1978], that is

$$X = \frac{1}{2}\left(1 - \frac{\bar{Q}}{BS_o c_k \Delta s}\right). \qquad (25)$$

The model routes surface runoff downstream, link by link, from the uppermost cell in the basin to the outlet, according to the network ordering system. The flood wave celerity $c_k = dQ/dA$, where Q is the discharge and A is the flow area, is expressed for each computational cell consisting of four grid points by applying the Manning-Gauckler-Strickler equation for rectangular channels with large width B, that is,

$$c_k = \frac{5}{3}k_S^{3/5}S_o^{3/10}B^{-2/5}\bar{Q}^{2/5}, \qquad (26)$$

where k_S is the Gauckler-Strickler roughness.

A similar scheme is applied to route local contributions to subsurface kinematic storm flow [*Beven and Germann*, 1982; *Beven*, 1982]. As shown in Figure 1, the unsaturated soil profile is lumped into two homogeneous units, representing a "root zone" and a "transmission zone." Soil hydraulic properties and moisture status are incorporated in the upper soil control volume to calculate the response g to the actual inflow f_i, via the conceptual equation (11), and a similar relationship can be applied to the transmission zone to calculate the local contributions to subsurface stormflow r in response to the inflow g. The kinematic wave approximation of saturated subsurface flow assumes that the flow lines in the saturated zone above the impermeable bed are parallel to the bed, and that the hydraulic gradient equals the slope of the bed. Local contributions to kinematic subsurface runoff from the transmission zone r are routed on a conceptual transport network extracted from DEM data via a routing scheme based on the Muskingum-Cunge method, where now Darcy's law is used instead of the Manning-Gauckler-Strickler equation [*Orlandini*, 1995].

Table 2. Vegetation and Soil Parameter Values for the Outlet and the Top Cells of the Rio Missiaga Basin

| Parameter	Outlet Value	Top Cell Value
z,* m	1100	2448
h, m	3.0	3.0
r_s, s m^{-1}	100	100
LAI	1	1
C, m	3×10^{-3}	3×10^{-3}
θ_r	0.04	0.04
θ_s	0.50	0.30
η	0.20	0.60
ψ_s, m	0.15	0.10
K_s, mm hr^{-1}	1.8	288.0
Z_{up}, m	0.30	0.30
Z_{low}, m	0.60	0.60

*Elevation above mean sea level.

5. Catchment Scale Application

In order to test the effects of the local soil water balance described in section 2.1 on the overall catchment storm flow response, a network routing model is applied to the Rio Missiaga experimental catchment, located on the western side of the Cordevole Valley (Belluno, Italy). The catchment's main geological features have been reported by *Friz et al.* [1983]. A 4.35-km^2 extension of the Rio Missiaga catchment was horizontally discretized into 1740 cells with a 50-m grid spacing (Figure 8). Surface cover and soil properties are assigned to each DEM cell. Although the model database is designed to incorporate a completely general set of parameter spatial distributions according to DEM and DTM information, to facilitate model calibration a functional relationship has been assumed for the parameter spatial distributions in this study. The distributions are expressed as exponential functions of the grid cell elevations, where the values of the top and outlet cell parameters are considered to characterize these distributions. The exponential relationship is

$$p_c = p_o \exp \left[- \frac{\ln (p_t/p_o)}{z_o - z_t} (z_c - z_o) \right], \qquad (27)$$

where p_c, p_o, and p_t represent the parameter values for an arbitrary cell, the outlet cell, and the top cell, respectively, and z_c, z_o, and z_t represent the corresponding cell elevations. The outlet and top cell values for elevation and for the model parameters are reported in Table 2 and represent reasonable values for the considered catchment area, although more extensive field data must be collected in order to fit and verify relationships such as (27) and in order to conduct a comprehensive model calibration and parameter optimization. In the simple application reported here the catchment response was calibrated by varying only the saturated conductivity K_s at the top cell of the catchment. Also, further study is required to investigate the effects of functional parameter distributions like (27) on simulation results.

The model was calibrated on the event shown in Figure 9 and validated on the events shown in Figures 10 and 11. We used a 1-hour time step (ΔT) for the local water balance and a 5-min time step to control the accuracy of the storm flow routing scheme. The calibration event shown in Figure 9 is reproduced by the model simulation in both the infiltration excess and kinematic subsurface runoff components. The rising limb and first peak of the hydrograph reflect surface runoff
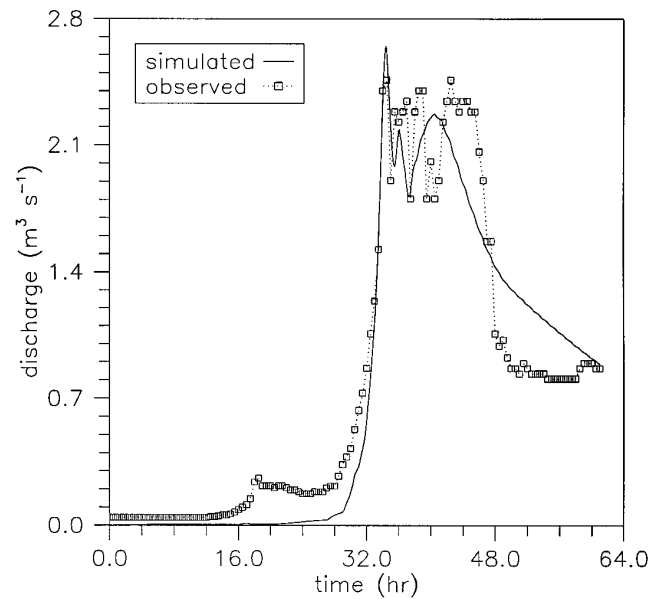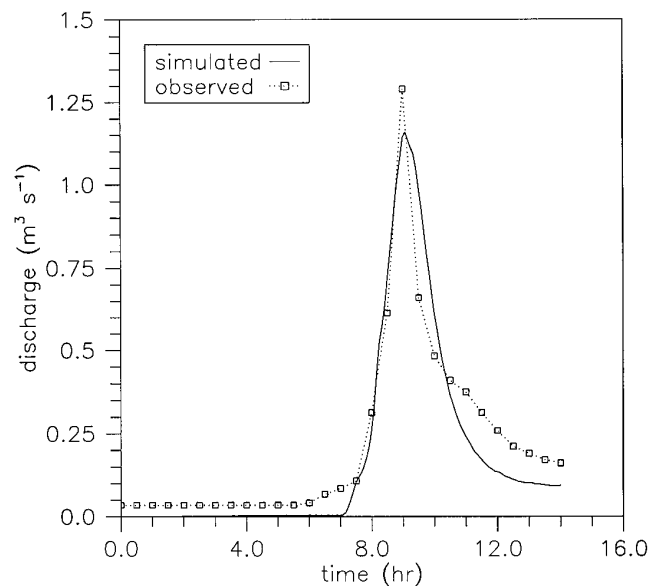

Figure 9. Comparison between simulated and observed outlet storm flows for the October 9–12, 1987, Rio Missiaga storm calibration event.

response, whereas successive peaks and the tail reflect kinematic subsurface storm flow response. As shown in Figures 10 and 11, the validation events are reasonably well simulated by the model. The hydrographs for the two validation events represent predominantly surface runoff response, as indicated by the single peaks of shorter duration and the shorter tails.
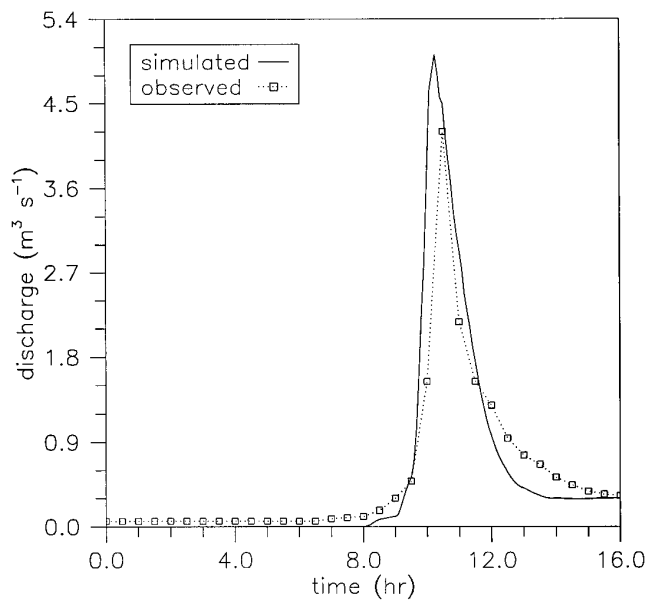
6. Summary and Conclusions

In this paper the response to storm events of a conceptual TCA-based water balance model of the upper unsaturated soil layer has been evaluated against a detailed Richards' equation

Figure 10. Comparison between simulated and observed outlet storm flows for the September 29, 1991, Rio Missiaga storm validation event.

Figure 11. Comparison between simulated and observed outlet storm flows for the September 14, 1993, Rio Missiaga storm validation event.

based on a one-dimensional finite element model. Both of these models are based on the same set of soil hydraulic properties (θ_r, θ_s, η, ψ_s, and K_s), and we have examined the sensitivities of the conceptual model response to scale representation, soil type, and moisture status, selecting Z_{up}, K_s, and Θ_i as representative parameters.

To determine the extent that the conceptual model is able to calculate the water balance of the upper soil layer, the base case parameter set used for the comparison runs represents severe conditions with respect to Z_{up}, K_s, and Θ_i. Where comparison between conceptual and detailed models was possible, the relative errors in cumulative control volume inflow and outflow were generally not greater than 20%. In addition, it was shown how, even for severe conditions on K_s and Θ_i, the conceptual model was able to describe the soil moisture dynamics for an upper soil layer of depth less than 0.10 m. Under severe conditions on Z_{up} and K_s, the model was able to reproduce the water balance of the soil control volume provided the initial moisture profile is sufficiently close to saturation ($\Theta_i \geq 70\%$). These results suggest that the conceptual model can be applied to describe the water balance of a two-layer unsaturated soil profile during storm periods. Under these conditions a thin control volume layer of depth $Z_{up} \approx 0.10$ m can be used to simulate the highly dynamical water flux partitioning at the land surface, whereas a thicker layer can be used to simulate the quasi-steady dynamics of the lower transmission zone.

The kinematic approximation applied to route local contributions to surface and subsurface runoff at the catchment scale was able to reproduce the storm flow response of the steeply sloping Rio Missiaga basin, although further work will be needed to improve the model's handling of subsurface catchment dynamics. Future work will compare the conceptual model and a detailed three-dimensional Richards equation–based finite element model to investigate local and catchment scale subsurface response and will test the validity of the idea of coupling the conceptual one-dimensional water balance

model, for the upper soil layers, to a detailed finite element flow model for the deeper soil layers.

References

Abbott, M. B., J. C. Bathurst, J. A. Cunge, P. E. O'Connell, and J. Rasmussen, An introduction to the European Hydrological System—Système Hydrologique Européen, "SHE", 1, History and philosophy of a physically-based, distributed modelling system, *J. Hydrol.*, *87*, 45–59, 1986.

Band, L. E., Topographic partition of watersheds with digital elevation models, *Water Resour. Res.*, *22*(1), 15–24, 1986.

Beven, K. J., On subsurface storm flow: Predictions with simple kinematic theory for saturated and unsaturated flows, *Water Resour. Res.*, *18*(6), 1627–1633, 1982.

Beven, K. J., and P. Germann, Macropores and water flow in soils, *Water Resour. Res.*, *18*(5), 1311–1325, 1982.

Binley, A., J. Elgy, and K. Beven, A physically based model of heterogeneous hillslopes, 1, Runoff production, *Water Resour. Res.*, *25*(6), 1219–1226, 1989.

Brooks, R. H., and A. T. Corey, Properties of porous media affecting fluid flow, *J. Irrig. Drain. Div. Am. Soc. Civ. Eng.*, *2*, 61–88, 1966.

Clarke, R. T., Mathematical models in hydrology, *Irrig. Drain. Rep. 19*, Food and Agric. Org., Rome, 1973.

Cunge, J. A., On the subject of a flood propagation computation method (Muskingum method), *J. Hydraul. Res.*, *7*(2), 205–230, 1969.

Eagleson, P. S., Climate, soil, and vegetation, 3, A simplified model of soil moisture movement in the liquid phase, *Water Resour. Res.*, *14*(5), 722–730, 1978.

Entekhabi, D., and P. S. Eagleson, Land surface hydrology parameterization for atmospheric general circulation models including subgrid scale variability, *J. Clim.*, *2*(8), 816–831, 1989.

Famiglietti, J. S., and E. F. Wood, Multiscale modeling of spatially variable water and energy balance processes, *Water Resour. Res.*, *30*(11), 3061–3078, 1994.

Freeze, R. A., Three-dimensional, transient, saturated-unsaturated flow in a groundwater basin, *Water Resour. Res.*, *7*(2), 347–366, 1971.

Friz, C., G. Gatto, V. Villi, and G. Caleffa, Groundwater resources of a typical catchment in the Dolomites area: The Rio Missiaga Catchment (Belluno, Italy) (in Italian), *Mem. Sc. Geol.*, *36*, 293–315, 1983.

Gan, T. Y., and S. J. Burges, An assessment of a conceptual rainfall-runoff model's ability to represent the dynamics of small hypothetical catchments, 1, Models, model properties, and experimental design, *Water Resour. Res.*, *26*(7), 1595–1604, 1990.

Ibrahim, H. A., and W. Brutsaert, Intermittent infiltration into soil with hysteresis, *J. Hydraul. Div. Am. Soc. Civ. Eng.*, *94*(1), 113–137, 1968.

Leopold, L. B., and T. Maddock Jr., The hydraulic geometry of stream channels and some physiographic implications, *Prof. Pap. 252*, U.S. Geol. Surv., Washington, D. C., 1953.

Milly, P. C. D., An event-based simulation model of moisture and energy fluxes at a bare soil surface, *Water Resour. Res.*, *22*(12), 1680–1692, 1986.

Milly, P. C. D., and P. S. Eagleson, Effects of spatial variability on average annual water balance, *Water Resour. Res.*, *23*(11), 2135–2141, 1987.

Orlandini, S., Space-time dependence of catchment-scale hydrologic processes: Comparison between physically based distributed models at different levels of conceptualization (in Italian), Ph.D. thesis, DIIAR, Politecnico di Milano, Milano, Italy, 1995.

Orlandini, S., and R. Rosso, Diffusion wave modeling of distributed catchment dynamics, *J. Hydraul. Eng.*, in press, 1996.

Paniconi, C., and E. F. Wood, A detailed model for simulation of

catchment scale subsurface hydrologic processes, *Water Resour. Res.*, 29(6), 1601–1620, 1993.

Paniconi, C., A. A. Aldama, and E. F. Wood, Numerical evaluation of iterative and noniterative methods for the solution of the nonlinear Richards equation, *Water Resour. Res.*, 27(6), 1147–1163, 1991.

Philip, J. R., The theory of infiltration, 7, *Soil Sci.*, 85, 333–337, 1958.

Philip, J. R., General method of exact solution of the concentration-dependent diffusion equation, *Aust. J. Phys.*, 13(1), 1–12, 1960.

Ponce, V. M., and V. Yevjevich, Muskingum-Cunge method with variable parameters, *J. Hydraul. Div. Am. Soc. Civ. Eng.*, 104(12), 1663–1667, 1978.

Protopapas, A. L., and R. L. Bras, The one-dimensional approximation for infiltration in heterogeneous soils, *Water Resour. Res.*, 27(6), 1019–1027, 1991.

Reeves, M., and E. E. Miller, Estimating infiltration for erratic rainfall, *Water Resour. Res.*, 11(1), 102–110, 1975.

Salvucci, G. D., and D. Entekhabi, Equivalent steady soil moisture profile and the time compression approximation in water balance modeling, *Water Resour. Res.*, 30(10), 2737–2749, 1994a.

Salvucci, G. D., and D. Entekhabi, Comparison of the Eagleson statistical-dynamical water balance model with numerical simulations, *Water Resour. Res.*, 30(10), 2751–2757, 1994b.

Salvucci, G. D., and D. Entekhabi, Hillslope and climatic controls on hydrologic fluxes, *Water Resour. Res.*, 31(7), 1725–1739, 1995.

Sloan, P. G., and I. D. Moore, Modeling subsurface storm flow on steeply sloping forested watersheds, *Water Resour. Res.*, 20(12), 1815–1822, 1984.

Smith, R. E., and R. H. B. Hebbert, Mathematical simulation of interdependent surface and subsurface hydrologic processes, *Water Resour. Res.*, 19(4), 987–1001, 1983.

Troch, P. A., M. Mancini, C. Paniconi, and E. F. Wood, Evaluation of a distributed catchment scale water balance model, *Water Resour. Res.*, 29(6), 1805–1817, 1993.

_____

M. Mancini, S. Orlandini, and R. Rosso, Dipartimento di Ingegneria Idraulica, Ambientale e del Rilevamento (DIIAR), Sezione Idraulica, Politecnico di Milano, Piazza Leonardo da Vinci 32, I-20133 Milano, Italy. (e-mail: mmancini@idra1.iar.polimi.it; stefano@idra1.iar.polimi.it; rr@idra1.iar.polimi.it)

C. Paniconi, Centro di Ricerca, Sviluppo e Studi Superiori in Sardegna (CRS4), Via Nazario Sauro 10, I-09123 Cagliari, Italy. (e-mail: cxpanico@crs4.it)